A Thiadiazole-capped Nanoribbon with 18 Linearly-Fused Rings

Diego Cortizo-Lacalle,[a] Cristian Gozalvez, [a] Manuel Melle-Franco,[b] Aurelio Mateo-Alonso*[a,c]

[a]*POLYMAT, University of the Basque Country UPV/EHU, Avenida de Tolosa 72, 20018, Donostia-San Sebastian, Spain. amateo@polymat.eu*
[b]*CICECO-Aveiro Institute of Materials, Department of Chemistry, University of Aveiro, 3810-193, Aveiro, Portugal.*
[c]*Ikerbasque, Basque Foundation for Science, E-48011 Bilbao, Spain.*

ABSTRACT: Polycyclic aromatic hydrocarbons that extend over 2 nm in one dimension are seen as monodisperse graphene nanoribbons, which have attracted significant attention for a broad range of applications in organic electronics and photonics. Herein we report the synthesis of a stable bisthiadiazole-capped pyrene-containing nanoribbon with an overall number of 18 linearly-fused rings (**NR-18-TD**). Thanks to the presence of alternating *tert*-butyl and tri-*iso*-butylsilyl groups, **NR-18-TD** is highly soluble in organic solvents and therefore it could be unambiguously characterized, its fundamental optoelectronic and redox properties could be established, and organic field-effect transistors were easily fabricated by liquid deposition. The characterization illustrates that **NR-18-TD** is a promising soluble NR-based *n*-type semiconductor for applications in organic electronics.

Introduction

Polycyclic aromatic hydrocarbons (PAHs) that extend over 2 nm in one dimension (1D) are seen as monodisperse graphene nanoribbons (NRs), which have attracted significant attention for a broad range of applications in organic electronics and photonics.[1] NRs combine the one-atom thickness of graphene with a tunable band gap that can be modulated by controlling the structure of the longitudinal edge, the length of the NR and heteroatom doping.

The synthesis of NRs with a precise edge and length is a challenging task because of long synthetic routes, which are often beset by insoluble and unstable compounds and intermediates. For example, acenes with 9 linearly-fused rings,[2] which can be considered the narrowest NR as they are about 2 nm in length, show a limited stability that do not allow device integration. Off-linear annulations increase the number of aromatic sextets in the acene framework and therefore provide longer and more stable monodisperse NRs, such as pyrene-[1c, 3] and coronene-fused NRs,[3c, 3d, 4] with a number of rings that oscillate between 9 and 30 linearly-fused rings. However, even if numerous potential applications have been foreseen, examples of monodisperse NR implemented in devices are scarce.[3b-d, 3h, 4b-d]

The introduction of heteroatoms such as N, O, S, P and B in the aromatic framework is also a promising approach to further fine-tune the electronic structure of NRs.[1f] For example, it is possible to change energy levels and supramolecular organization by varying the number and position of N atoms in the aromatic framework.[5] In these terms, the incorporation of benzothiadiazole rings in the structure of PAHs is a promising approach for developing electron-deficient compounds for NIR absorbing and emitting applications, organic photovoltaics and organic field-effect transistors (OFETs).[6]

Although some efforts have been dedicated to the synthesis and characterization of pyrene-fused acenes incorporating thiadiazoles with promising results,[3b, 7] extended 1D structures thereof with >9 rings have not been synthesized and remain unexplored to date. Herein, we report the synthesis of a stable bisthiadiazole-capped pyrene-containing NR with an overall number of 18 linearly-fused rings (**NR-18-TD**) that shows alternating tri-*iso*-butylsilyl and *tert*-butyl substituents. The high solubility of **NR-18-TD** allowed establishing unambiguously its structure and properties by a combination of ^{1}H-NMR, ^{13}C-NMR, high-resolution mass spectrometry, absorption and photoluminescence spectroscopies and cyclic voltammetry. Furthermore, such enhanced solubility also allowed the fabrication of OFETs by liquid deposition, which illustrate that **NR-18-TD** is a promising soluble NR-based *n*-type semiconductor.

Results and discussion

Synthetic procedures. The synthesis of **NR-18-TD** was accomplished by a double cyclocondensation reaction between **NR-10-Q** and diaminobenzothiadiazole **BTD-NH$_2$** (Scheme 1). **NR-10-Q** was synthesized from precursors **A** and **B** in 2 steps according to a reported procedure.[3a] **A** and **B** were synthesised in 12 and 2 steps, respectively, while **BTD-NH$_2$**[3a] was prepared in 5 steps. When, **NR-10-Q** and **BTD-NH$_2$** were refluxed in a mixture of $CHCl_3$ and acetic acid under nitrogen, the reaction color changed gradually within five hours from dark purple to bright emissive purple evidencing the progress of the reaction. **NR-18-TD** could be easily isolated by column chromatography and was obtained in a good yield (38-56%) as a purple solid that is readily soluble in low boiling point organic solvents such as CH_2Cl_2, $CHCl_3$, toluene, and tetrahydrofuran. This enhanced solubility is a consequence of the alternating *tert*-butyl and tri-*iso*-butylsilyl groups, which have proven to be very efficient in the solubilisation of longer NRs.[3a] In addition, **NR-18-TD** showed a good stability under ambient conditions and was stored as a solid at room temperature for months without showing any evidence of decomposition.

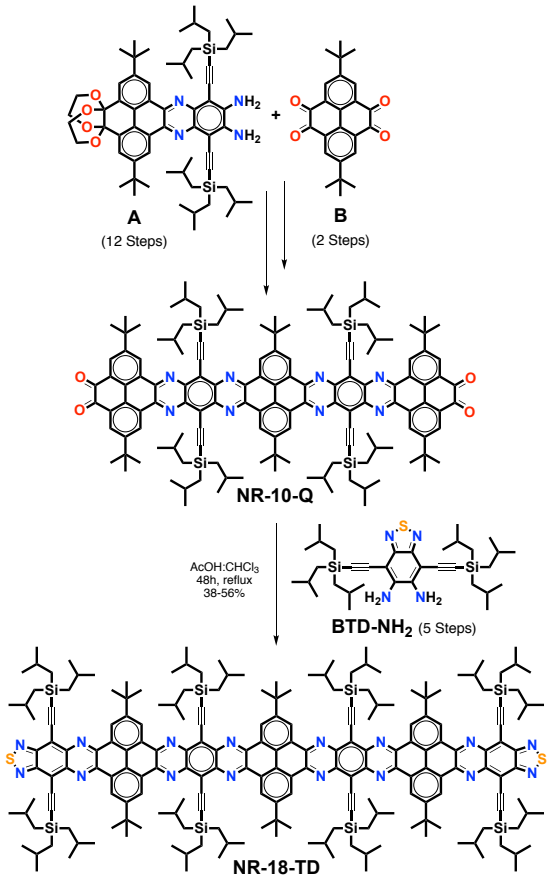

Scheme 1. Synthesis of **NR-18-TD**.

Structural Charaterisation. Thanks to the excellent solubility in organic solvents, **NR-18-TD** was unambiguously characterized by ^{1}H-NMR, ^{13}C-NMR, high-resolution matrix-assisted laser desorption/ionisation time of flight mass spectroscopy (MALDI-TOF HRMS), and UV-vis-NIR absorption and photoluminescence. ^{1}H-NMR and ^{13}C-NMR spectra showed sharp and well-resolved peaks in $CDCl_3$ at room temperature that are consistent with the structure (Figure S1 and Figure S2). HRMS show the expected molecular ion peak $(M+Ag)^+$ and isotopic distributions for **NR-18-TD** (Figure S3). Although **NR-18-TD** tend to form small crystals, we were unable to obtain crystals suitable for X-ray diffraction and calculated the structure with computer modelling (B3LYP-6-31g(d,p)) in order to get an insight on the geometry and the dimensions (Figure 1). From the calculations, we can conclude that although some localized twists are possible, the geometry of **NR-18-TD** is only slightly deviated from planarity, given the large flexibility of the substituents. **NR-18-TD** is approximately 4.3 nm long.

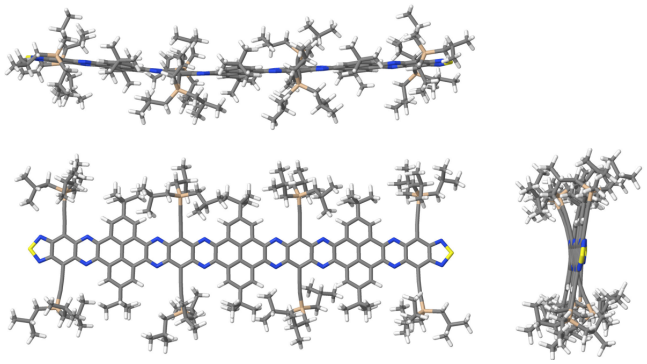

Figure 1. Three perspectives of the calculated structure of **NR-18-TD** at the B3LYP-6-31g(d,p) level.

Optoelectronic Characterisation. The optical properties of **NR-18-TD** were investigated by UV-vis-NIR absorption and photoluminescence spectroscopies in solution (Figure 2). The absorption spectrum of **NR-18-TD** in CH_2Cl_2 shows well-resolved bands with vibronic features in some cases. In particular, intense absorption bands with maxima at 264 (log ε = 5.24), 368 (log ε = 5.18), 538 (log ε = 5.27) and 601 nm (log ε = 4.39), which were assigned to the *β'*, *β*, *ρ* and *α* bands, respectively, in agreement with previous reports.[3a, 8] The *ρ* band of **NR-18-TD** (538 nm) appears red-shifted in comparison to a bisthiadiazole analogue with 8 linearly-fused rings (528 nm)[6b] and blue-shifted in comparison to a longer pyrene-containing NR with 20 linearly-fused rings (544 nm).[3a] This is consistent with the direct relationship between the *ρ* band and the linear conjugation. While the of *α* band remains invariable at 604 independently of the length in agreement with previous work on this family of pyrene-containing NR.[3a, 6b]

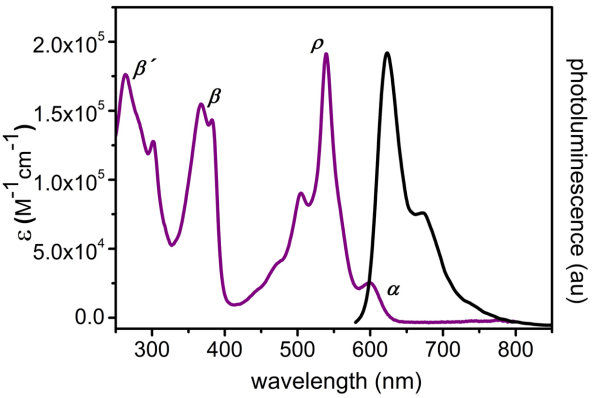

Figure 2. UV-visible absorption (purple) and emission (black) spectra of **NR-18-TD** in CH_2Cl_2.

To understand the nature of the electronic transitions, the absorption spectra of **NR-18-TD** was computed with TD-DFT with the 6–31g(d,p) basis set with the B3LYP Hamiltonian. Two peaks were obtained in the simulation, a weaker peak (*α*) and an intense peak (*ρ)*. The *α* peak appears in the range 640-680 nm and arises from electronic transitions between the four quasi-degenerate HOMOs and the four quasi-degenerate LUMOs (Tables S1 and S2). The intense *ρ* peak is due to a very intense transition at ~ 550 nm, from the excitation of, mostly, electrons from the HOMO-4 level, which is the first non-degenerated level (Table S1). These two peaks have maxima at 646 and 550 nm, which compare well with the experimental values of 604 and 544 nm.

The photoluminescence was also investigated in CH_2Cl_2 (Figure 2). Independently of the excitation wavelength, **NR-18-TD** showed a broad emission band from 600 nm to the near infrared, *ca* 775 nm, with a maximum at 623 nm and a shoulder at 672 nm, which is again comparable to a bisthiadiazole analogue with 8 linearly-fused rings (528 nm)[6b] and with longer pyrene-containing NR with 20 linearly-fused rings (544 nm)[3a] as the emission evolved from the *α* band.

Electrochemistry. The redox properties of **NR-18-TD** were studied by cyclic voltammetry in CH_2Cl_2 using tetrabutylammonium hexafluorophosphate (nBu$_4$NPF$_6$) (0.1 M) as the supporting electrolyte (Figure 3). All the potential values were referenced. Upon reduction, **NR-18-TD** showed three reversible peaks at $E_{1/2}^{I}$ = –0.96, $E_{1/2}^{II}$ = –1.09 and $E_{1/2}^{III}$ = –1.56 V *versus* the ferrocenium/ferrocene couple. On the oxidative scan, no redox processes were observed within the solvent-supported electrolyte window. The $E_{1/2}^{I}$ for **NR-18-TD** is low in comparison with the longest pyrene-containing NR with 30 linearly-fused rings ($E_{1/2}^{I}$ = –1.18 V),[3a] which confirms that the incorporation of two thiadiazoles

on the aromatic backbone of the NRs is a promising approach for developing electron-deficient compounds.

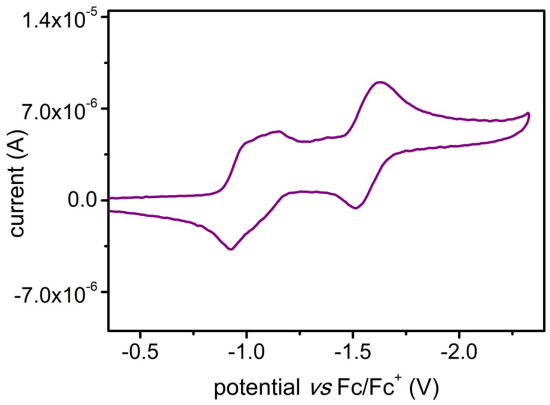

Figure 3. Cyclic voltammogram of **NR-18-TD** in a 0.1 M solution of nBu$_4$NPF$_6$ in CH_2Cl_2.

Energy levels. The HOMO-LUMO gap (E_g = 1.97 eV) was calculated from the onset of the longest wavelength absorption (α) band. This value is the same as the HOMO-LUMO gap of a bisthiadiazole analogue with 8 linearly-fused rings (E_g = 1.97 eV)[6b] or the longest pyrene-containing NR with 30 linearly-fused rings (E_g = –1.97 eV),[3a] since the α band remains at the same energy independently of the length, at least for NR with <30 rings.[3a] The electrochemical LUMO level or electron affinity (E_{LUMO}) was estimated from the onset of the first reduction process (E_{LUMO} = –3.91 eV) and was found to be lower than that of longest pyrene-containing NR with 30 linearly-fused rings (E_{LUMO} = –3.69 eV)[3a] even if **NR-18-TD** is shorter. This is the result of the incorporation of the thiadiazole rings. The HOMO level (E_{HOMO} = –5.89 eV) was estimated from the electrochemical LUMO level and the HOMO-LUMO gap. These values are in accordance with calculated energy levels (E_{LUMO} = –3.41 eV; E_{HOMO} = –5.50 eV) at the B3LYP-6-31g(d,p) level. A comparison of the calculated energy levels for the frontier orbitals between **NR-18-TD** and the flat **NR-18-TD-H** (a **NR-18-TD** virtual derivative in which the TIBS groups have been substituted by H) reveal that the planarity deformations have little effect on the energy levels with differences of 0.23-0.25 eV for the HOMOs and 0.1-0.12 eV for the LUMOs (Figures S4-S6 and Table S2).

Electrical Characterisation. The charge transport properties of **NR-18-TD** were evaluated in OFETs. Again, the excellent solubility of **NR-18-TD** in organic solvents allowed it to be easily deposited by liquid methods in a bottom-gate bottom-contact architecture (with pre-patterned Au contacts) on a SiO_2 substrate

(230 nm thick thermally oxidized SiO_2 on Si), which had been previously passivated by introducing a monolayer of octadecyltrichlorosilane (OTS) through a wet process. **NR-18-TD** was deposited on top by either spin coating or dropcasting using $CHCl_3$ and toluene (Table S3) inside a glovebox. Finally, the samples were annealed (80ºC and 160ºC) under inert atmosphere. Electrical characterization of the devices showed a typical behavior for *n*-type semiconductors (Figure 4 and Table S3). As expected, **NR-18-TD** did not show hole transport. The average electron mobilities (μ_e) obtained for spin-coated thin films using $CHCl_3$ and annealing at 80 °C were $\mu_e = 5.5\times10^{-6}$ $cm^2V^{-1}s^{-1}$ with a maximum electron mobility (μ_e^{max}) of 9.4×10^{-6} $cm^2V^{-1}s^{-1}$ The μ_e and μ_e^{max} values increased about an order of magnitude after annealing at 160 ºC ($\mu_e = 3.9\times10^{-5}$ $cm^2V^{-1}s^{-1}$; $\mu_e^{max} = 6.6\times10^{-5}$ $cm^2V^{-1}s^{-1}$). Higher μ_e and μ_e^{max} values were observed for **NR-18-TD** thin films deposited by spin coating toluene solutions upon annealing at 80 ºC ($\mu_e = 1.8\times10^{-5}$ $cm^2V^{-1}s^{-1}$; $\mu_e^{max} = 4.4\times10^{-5}$ $cm^2V^{-1}s^{-1}$) in comparison to $CHCl_3$ under the same conditions. The μ_e and μ_e^{max} values were also improved upon annealing at 160 ºC ($\mu_e = 5.2\times10^{-5}$ $cm^2V^{-1}s^{-1}$; $\mu_e^{max} = 1.0\times10^{-4}$ $cm^2V^{-1}s^{-1}$). OFETs fabricated from dropcasted thin films from toluene showed similar $\mu_e = 4.5\times10^{-5}$ $cm^2V^{-1}s^{-1}$and the highest $\mu_e^{max} = 1.4\times10^{-4}$ $cm^2V^{-1}s^{-1}$ upon annealing at 160 ºC without any device optimization.

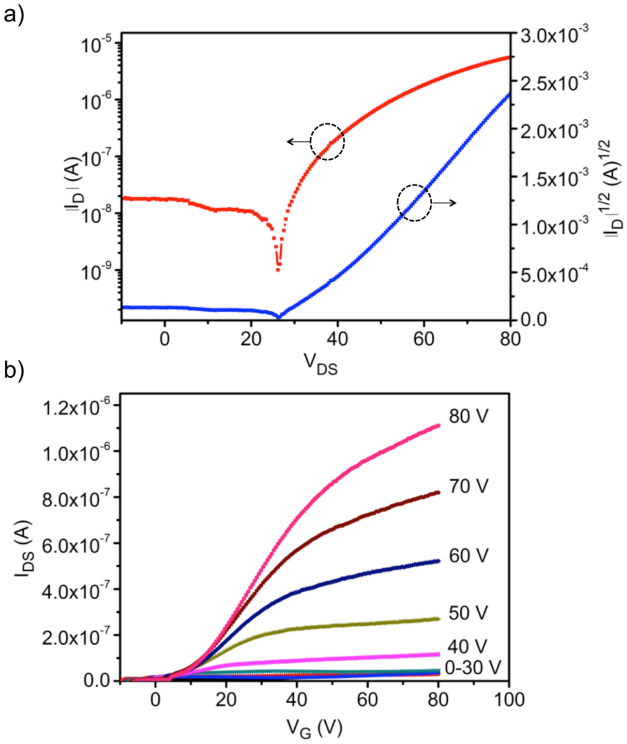

Figure 4. Representative a) transfer and b) output curve characteristics for **NR-18-TD** in a bottom-contact bottom gate configuration measured under inert atmosphere (W=10000 μm, L=2.5 μm).

Conclusions

To conclude, we have reported the synthesis and characterisation of a pyrene-containing NR end-capped with two thiadiazole rings (**NR-18-TD**). Thanks to the presence of alternating *tert*-butyl and TIBS groups, **NR-18-TD** is highly soluble in organic solvents and therefore it could be unambiguously characterized, its fundamental optoelectronic and redox properties could be established, and OFETs were easily fabricated by liquid deposition methods. The optoelectronic and electrochemical characterization shows that the incorporation of thiadiazole rings in both ends lowers the LUMO level of **NR-18-TD** (–3.91 eV) to values beyond those of longest pyrene-containing NR with 30 linearly-fused rings.[3a] Electrical characterization of thin films of **NR-18-TD** deposited from solution show a *n*-type behavior and a maximum electron mobility of $\mu_e^{max} = 1.4\times10^{-4}\ cm^2V^{-1}s^{-1}$ without any device optimization. Our results show that the incorporation of two thiadiazoles at the both ends of the aromatic backbone of pyrene-containing NRs with alternating solubilizing groups is a promising approach for developing soluble NR-based *n*-type semiconductors for applications in organic electronics.

Acknowledgements

We are grateful to the Basque Science Foundation for Science (Ikerbasque), POLYMAT, the University of the Basque Country (Grupo de Investigación GIU17/054 and SGIker), Gobierno de España (Ministerio de Economía y Competitividad CTQ2016-77970-R and CTQ2015-71936-REDT), Gobierno Vasco (BERC program), CICECO-Aveiro Institute of Materials, POCI-01-0145-FEDER-007679 (FCT ref. UID/CTM/50011/2013), Diputación Foral de Guipúzcoa (OF215/2016(ES)) and the FP7 framework program of the European Union (Marie Curie Career Integration Grant No. 618247 (NIRVANA)). This project has received funding from the European Union's Horizon 2020 research and innovation programme under grant agreement No 664878. This project has received funding from the European Research Council (ERC) under the European Union's Horizon 2020 research and innovation programme (grant agreement n° 722951).

References

1. (a) M. Fujita, K. Wakabayashi, K. Nakada and K. Kusakabe, *J. Phys. Soc. Jpn.*, 1996, **65**, 1920-1923; (b) L. Chen, Y. Hernandez, X. Feng and K. Müllen, *Angew. Chem. Int. Ed.*, 2012, **51**, 7640-7654; (c) A. Mateo-Alonso, *Chem. Soc. Rev.*, 2014, **43**, 6311-6324; (d) Z. Fei, M. D. Goldflam, J. S. Wu, S. Dai, M. Wagner, A. S. McLeod, M. K. Liu, K. W. Post, S. Zhu, G. C. A. M. Janssen, M. M. Fogler and D. N. Basov, *Nano Lett.*, 2015, **15**, 8271-8276; (e) X. Meng, C. Yu, X. Song, Y. Liu, S. Liang, Z. Liu, C. Hao and J. Qiu, *Adv. Energy Mater.*, 2015, **5**,

1500180; (f) M. Stępień, E. Gońka, M. Żyła and N. Sprutta, *Chemical Reviews*, 2017, **117**, 3479-3716.
2. (a) I. Kaur, M. Jazdzyk, N. N. Stein, P. Prusevich and G. P. Miller, *J. Amer. Chem. Soc.*, 2010, **132**, 1261-1263; (b) B. Purushothaman, M. Bruzek, S. R. Parkin, A.-F. Miller and J. E. Anthony, *Angew. Chem. Int. Ed.*, 2011, **50**, 7013-7017; (c) R. Huang, H. Phan, T. S. Herng, P. Hu, W. Zeng, S.-q. Dong, S. Das, Y. Shen, J. Ding, D. Casanova and J. Wu, *J. Amer. Chem. Soc.*, 2016, **138**, 10323-10330; (d) J. Krüger, F. García, F. Eisenhut, D. Skidin, J. M. Alonso, E. Guitián, D. Pérez, G. Cuniberti, F. Moresco and D. Peña, *Angew. Chem. Int. Ed.*, 2017, **56**, 11945-11948.
3. (a) D. Cortizo-Lacalle, J. P. Mora-Fuentes, K. Strutyński, A. Saeki, M. Melle-Franco and A. Mateo-Alonso, *Angew. Chem. Int. Ed.*, 2018, **57**, 703-708; (b) Z. Wang, P. Gu, G. Liu, H. Yao, Y. Wu, Y. Li, G. Rakesh, J. Zhu, H. Fu and Q. Zhang, *Chem. Commun.*, 2017, **53**, 7772-7775; (c) T. J. Sisto, Y. Zhong, B. Zhang, M. T. Trinh, K. Miyata, X. Zhong, X. Y. Zhu, M. L. Steigerwald, F. Ng and C. Nuckolls, *J. Amer. Chem. Soc.*, 2017, **139**, 5648-5651; (d) Y. Zhong, T. J. Sisto, B. Zhang, K. Miyata, X. Y. Zhu, M. L. Steigerwald, F. Ng and C. Nuckolls, *J. Amer. Chem. Soc.*, 2017, **139**, 5644-5647; (e) B. Kohl, F. Rominger and M. Mastalerz, *Angew. Chem. Int. Ed.*, 2015, **54**, 6051-6056; (f) K. Ozaki, K. Kawasumi, M. Shibata, H. Ito and K. Itami, *Nat. Commun.*, 2015, **6**, 6251; (g) B. Gao, M. Wang, Y. Cheng, L. Wang, X. Jing and F. Wang, *J. Amer. Chem. Soc.*, 2008, **130**, 8297-8306; (h) P.-Y. Gu, Z. Wang, G. Liu, H. Yao, Z. Wang, Y. Li, J. Zhu, S. Li and Q. Zhang, *Chemistry of Materials*, 2017, **29**, 4172-4175.
4. (a) E. Castro, T. J. Sisto, E. L. Romero, F. Liu, S. R. Peurifoy, J. Wang, X. Zhu, C. Nuckolls and L. Echegoyen, *Angew. Chem. Int. Ed.*, 2017, **56**, 14648-14652; (b) A. H. Endres, M. Schaffroth, F. Paulus, H. Reiss, H. Wadepohl, F. Rominger, R. Krämer and U. H. F. Bunz, *J. Amer. Chem. Soc.*, 2016, **138**, 1792-1795; (c) Y. Zhong, M. T. Trinh, R. Chen, G. E. Purdum, P. P. Khlyabich, M. Sezen, S. Oh, H. Zhu, B. Fowler, B. Zhang, W. Wang, C.-Y. Nam, M. Y. Sfeir, C. T. Black, M. L. Steigerwald, Y.-L. Loo, F. Ng, X. Y. Zhu and C. Nuckolls, *Nat. Commun.*, 2015, **6**, 8242; (d) Y. Zhong, B. Kumar, S. Oh, M. T. Trinh, Y. Wu, K. Elbert, P. Li, X. Zhu, S. Xiao, F. Ng, M. L. Steigerwald and C. Nuckolls, *J. Amer. Chem. Soc.*, 2014, **136**, 8122-8130; (e) Y. Fogel, M. Kastler, Z. Wang, D. Andrienko, G. J. Bodwell and K. Müllen, *J. Amer. Chem. Soc.*, 2007, **129**, 11743-11749.
5. (a) Q. Miao, T.-Q. Nguyen, T. Someya, G. B. Blanchet and C. Nuckolls, *Journal of the American Chemical Society*, 2003, **125**, 10284-10287; (b) Q. Miao, *Advanced Materials*, 2014, **26**, 5541-5549; (c) Z. Liang, Q. Tang, J. Xu and Q. Miao, *Advanced Materials*, 2011, **23**, 1535-1539; (d) A. Naibi Lakshminarayana, A. Ong and C. Chi, *Journal of Materials Chemistry C*, 2018, **6**, 3551-3563; (e) J. Li and Q. Zhang, *ACS Applied Materials & Interfaces*, 2015, **7**, 28049-28062; (f) J. E. Anthony, *Chemical Reviews*, 2006, **106**, 5028-5048; (g) K. E. Maly, *Crystal Growth & Design*, 2011, **11**, 5628-5633.

6. (a) T. C. Parker, D. G. Patel, K. Moudgil, S. Barlow, C. Risko, J.-L. Bredas, J. R. Reynolds and S. R. Marder, *Materials Horizons*, 2015, **2**, 22-36; (b) D. Cortizo-Lacalle, A. Pertegas, M. Melle-Franco, H. J. Bolink and A. Mateo-Alonso, *Organic Chemistry Frontiers*, 2017, **4**, 876-881.
7. (a) P.-Y. Gu, J. Zhang, G. Long, Z. Wang and Q. Zhang, *Journal of Materials Chemistry C*, 2016, **4**, 3809-3814; (b) A. B. Marco, D. Cortizo-Lacalle, C. Gozalvez, M. Olano, A. Atxabal, X. Sun, M. Melle-Franco, L. E. Hueso and A. Mateo-Alonso, *Chem. Commun.*, 2015, **51**, 10754-10757; (c) L. V. Brownell, K. A. Robins, Y. Jeong, Y. Lee and D.-C. Lee, *The Journal of Physical Chemistry C*, 2013, **117**, 25236-25247; (d) L. V. Brownell, K. Jang, K. A. Robins, I. C. Tran, C. Heske and D.-C. Lee, *Phys. Chem. Chem. Phys.*, 2013, **15**, 5967-5974; (e) M. Luo, H. Shadnia, G. Qian, X. Du, D. Yu, D. Ma, J. S. Wright and Z. Y. Wang, *Chem. Eur. J.*, 2009, **15**, 8902-8908.
8. E. Clar, *The Aromatic Sextet*, Wiley, London, 1972.